Figures and Legends

Figure 1. Diagrammatic representation of the development of the eye in a generalized vertebrate. **A:** Five brain vesicles and spinal cord. The optic vesicles evaginate from the wall of the diencephalon. **B:** The development of the eye. The optic vesicle invaginates to form a double-layered optic cup. Lens placode is made from the overlying ectoderm. The optic cup develops the neural retina and pigmented epithelium as the lens is internalized.

A

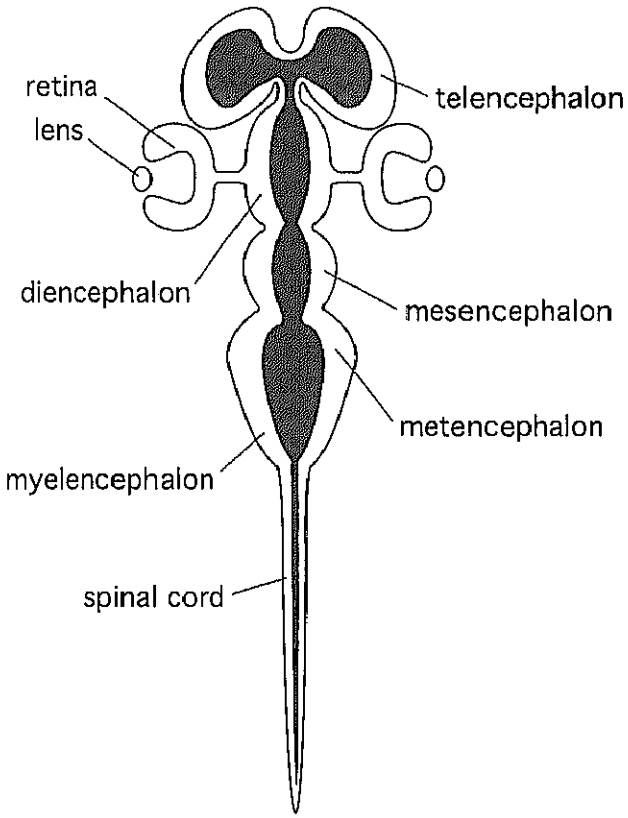
retina
lens
telencephalon
diencephalon
mesencephalon
metencephalon
myelencephalon
spinal cord

B

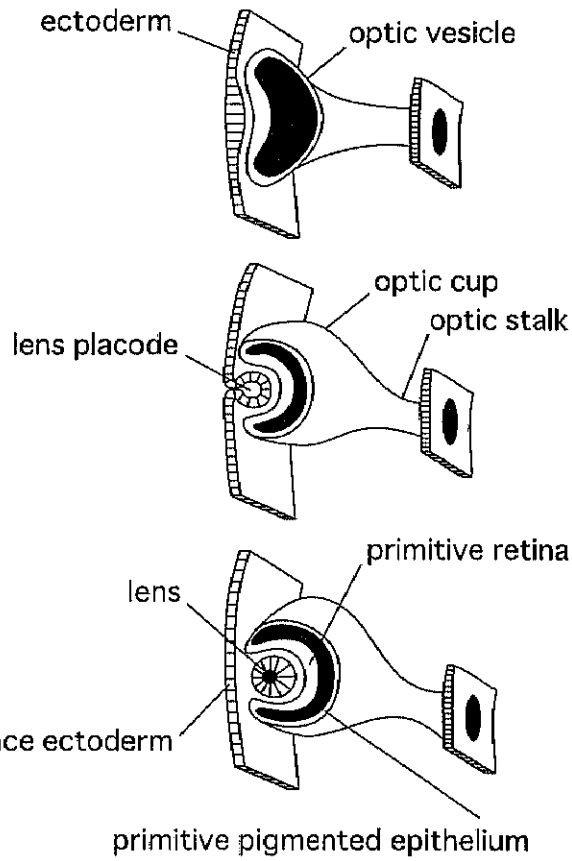
ectoderm
optic vesicle
optic cup
optic stalk
lens placode
primitive retina
lens
surface ectoderm
primitive pigmented epithelium

Figure 2. Schematic diagram showing typical retinal neurons of the fish and organization of retinal layers. R, rod photoreceptor cell; C, cone photoreceptor cell; H, horizontal cell; B, bipolar cell; A, amacrine cell; G, ganglion cell; RCL, receptor cell layer; ONL, outer nuclear layer; OPL, outer plexiform layer; INL, inner nuclear layer; IPL, inner plexiform layer; GCL, ganglion cell layer.

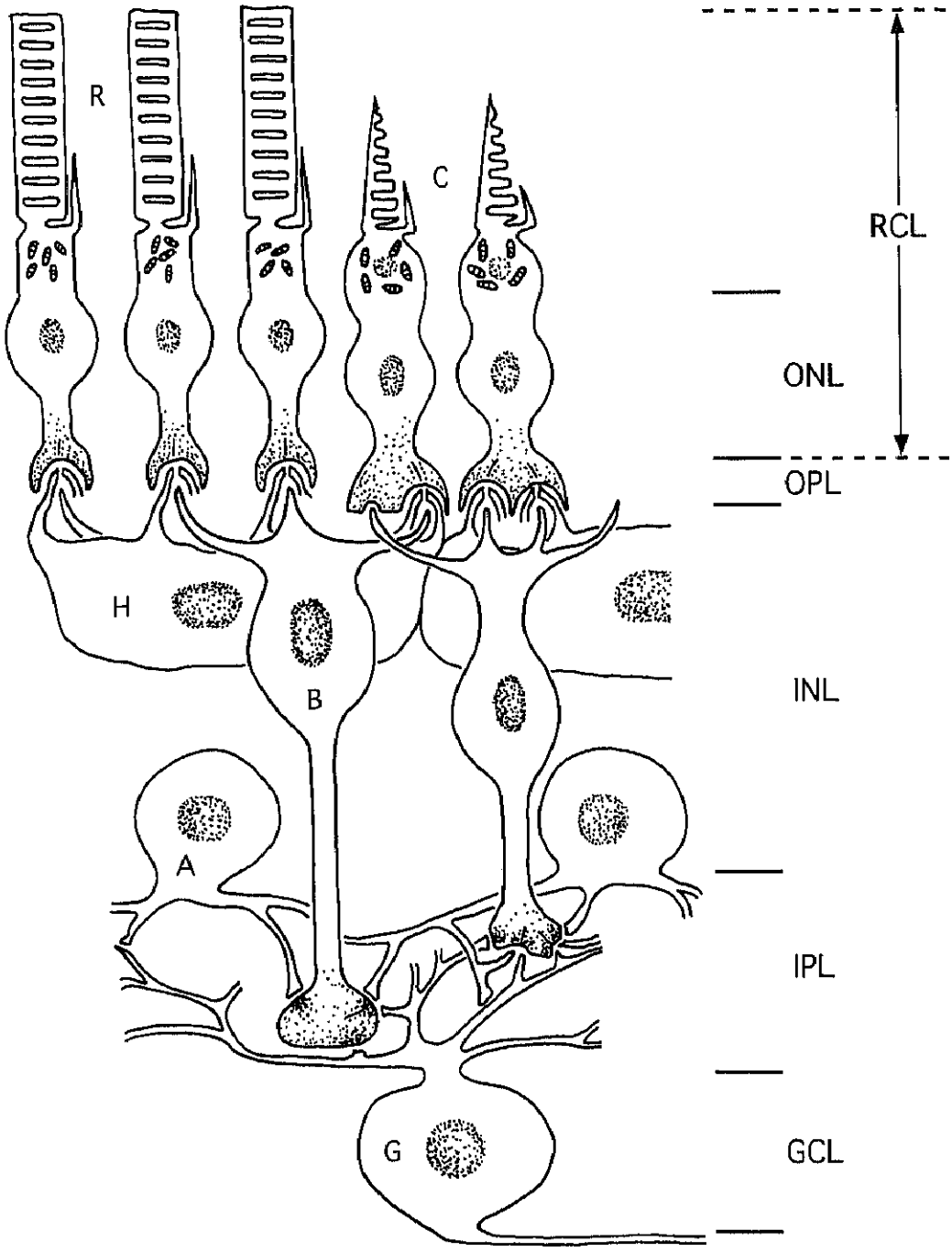
R
C
H
B
A
G
RCL
ONL
OPL
INL
IPL
GCL

Figure 3. Outline of procedures for making the living slice preparations including the peripheral retina. **A:** An eyeball was opened up along the dotted line. **B:** The lens and the cornea were removed. A piece of the temporal parts of the retina was cut along the dotted line and transferred to a filter paper. **C:** A piece of cut six sectors were mounted on the filter paper so as to be vitreous-side-down. **D:** The sclera and the pigmented epithelium were peeled gently. **E:** The retina with filter paper was transretinally sliced at a thickness of 200 μm. **F:** The sliced retinas were carried to a perfusion chamber. **G:** Slice preparation including the peripheral retina fixed on the cover glass by Vaseline at the both ends of filter paper.

A

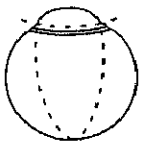

eyeball

B

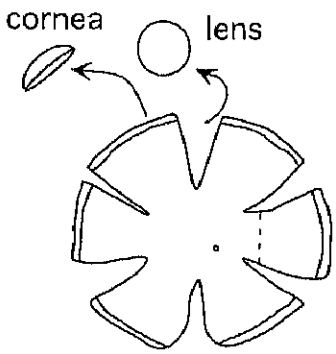

C

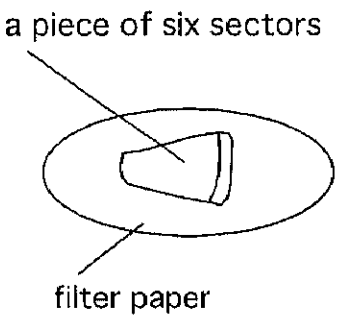

D

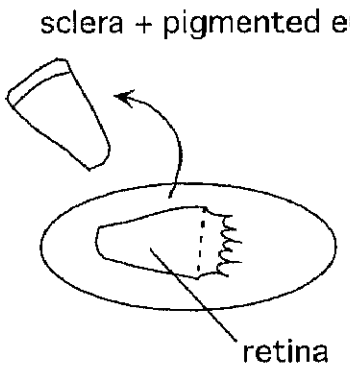

E

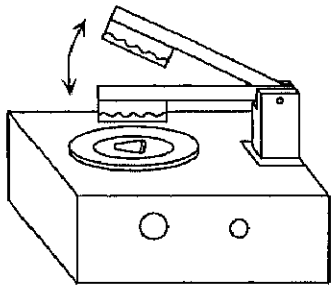

chopper

F

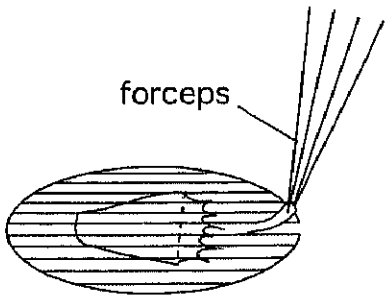

G

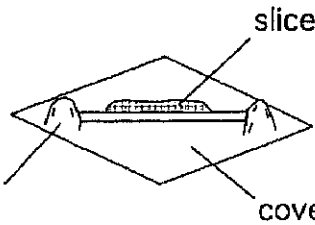

Figure 4. Schematic diagram of whole-cell patch-clamp recording system. The chamber was mounted on upright microscope stage. Experimental solutions (listed in Table 2) were continuously supplied by gravity through inlet tube (*inlet*) and sucked out through outlet tube (*outlet*). A reference electrode was connected to the experimental solutions via 3M KCl agar bridge. A cell was made a whole-cell configuration with a patch pipette by a gentle suction (see Fig. 5). The patch pipette was filled with an isotonic pipette solution (listed in Table 1). Whole-cell current detected by a recording electrode was amplified by a patch-clamp amplifier (*OA*) and monitored. The data were stored on computer hard disk.

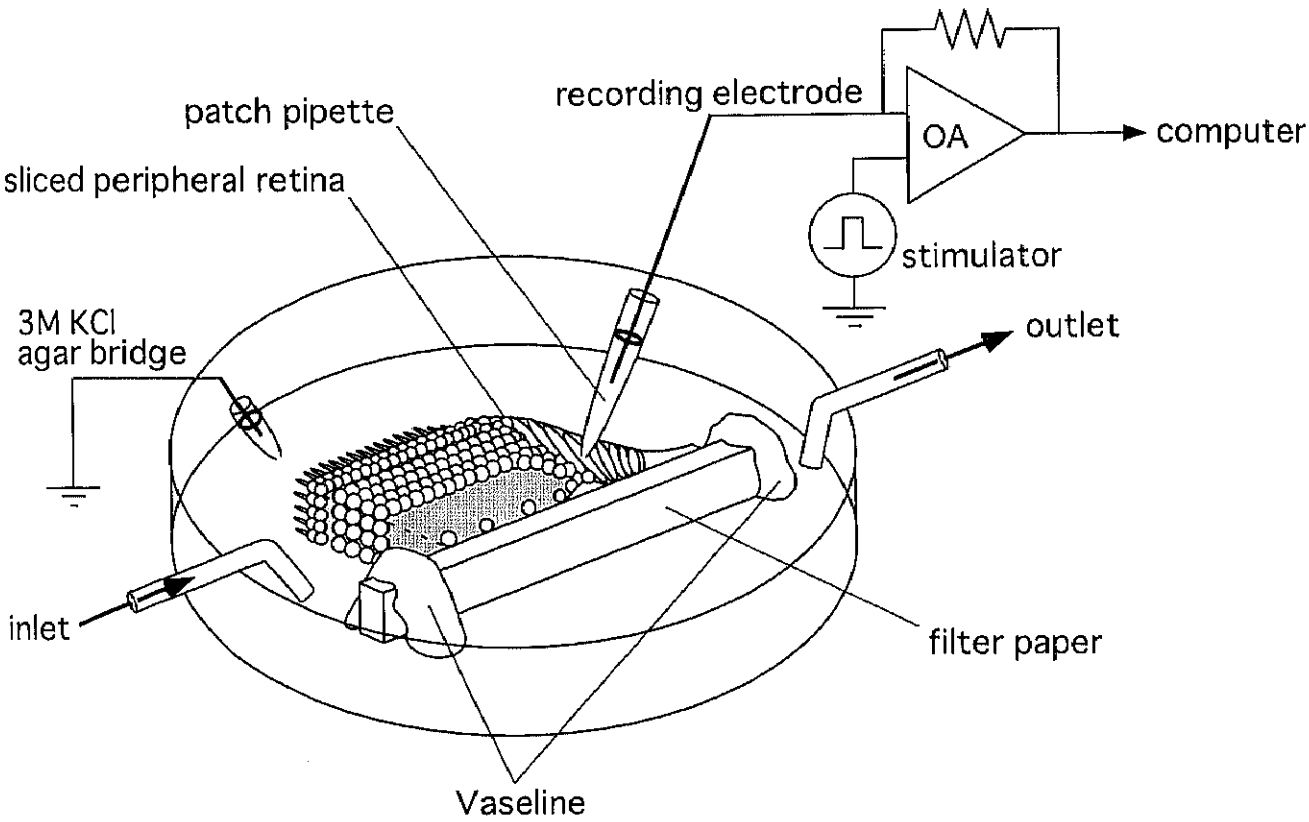
recording electrode
patch pipette
sliced peripheral retina
OA
computer
stimulator
3M KCl
agar bridge
outlet
inlet
filter paper
Vaseline

Figure 5. Conventional ruptured whole-cell patch-clamp methods. **A:** Neurons express various ion channels, such as K^+, Ca^{2+} and Na^+ channels. **B:** A pipette tip touches on the cell membrane to form a gigaohm-seal. Membrane patch is ruptured by suction. **C:** Whole-cell currents through ion channels are recorded.

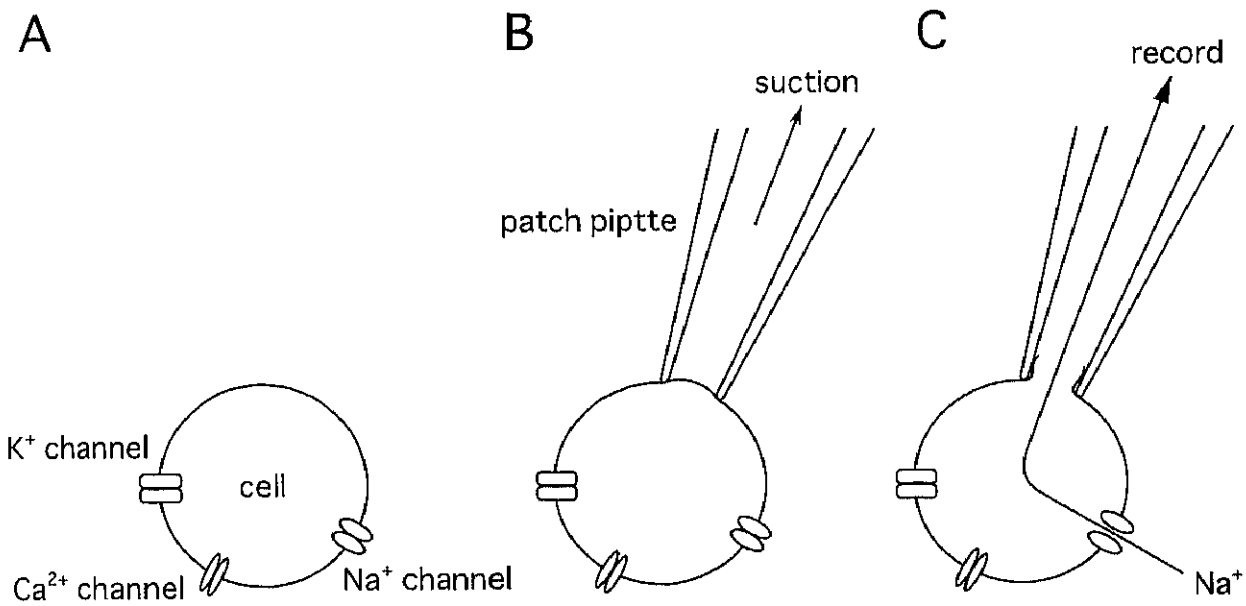
A
B
C
suction
record
patch piptte
K+ channel
cell
Ca2+ channel
Na+ channel
Na+

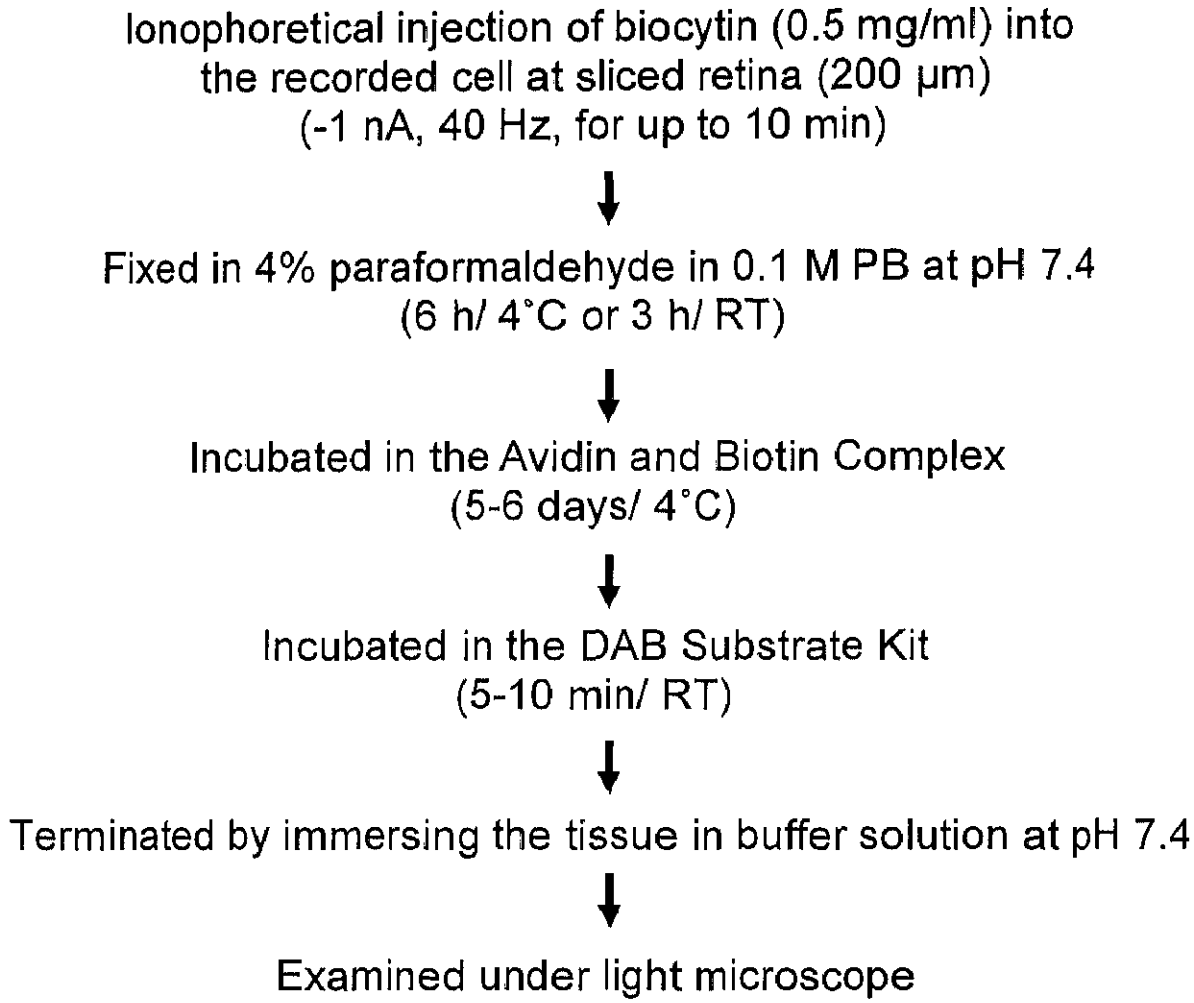

Figure 6. Procedures of intracellular staining of marginal progenitor cells through gap junction.

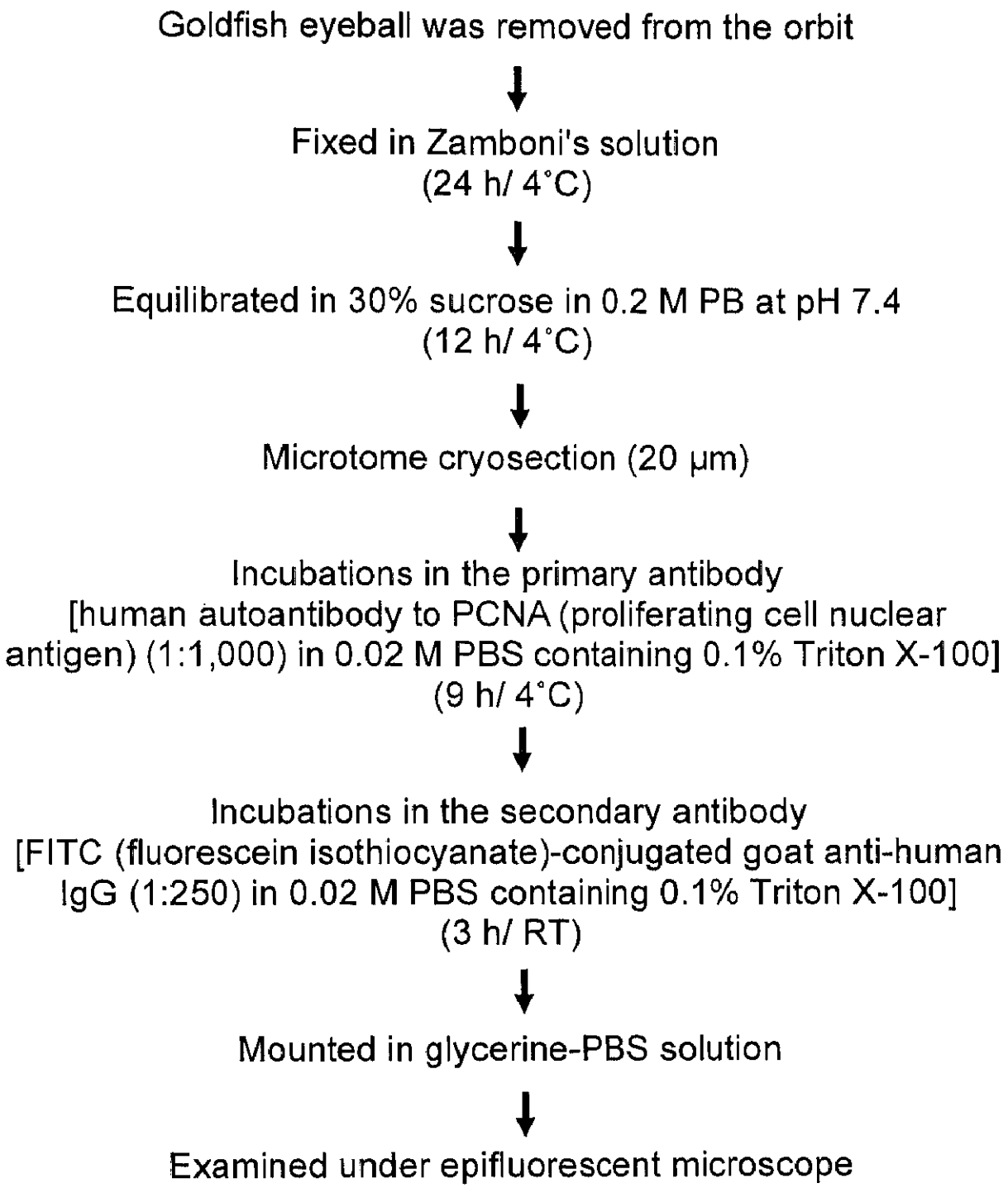

Figure 7. Sequence of steps in the immunohistochemical localization of progenitor cells.

Figure 8. Anatomy of the adult goldfish eye and the structure of the peripheral retina. **A:** A transverse paraffin section of an adult goldfish eye stained with toluidine blue. **B:** Peripheral retina at higher magnification of red square region in A. RPE, retinal pigmented epithelium; BV, blood vessel. Other abbreviations are the same as those in Figure 2.

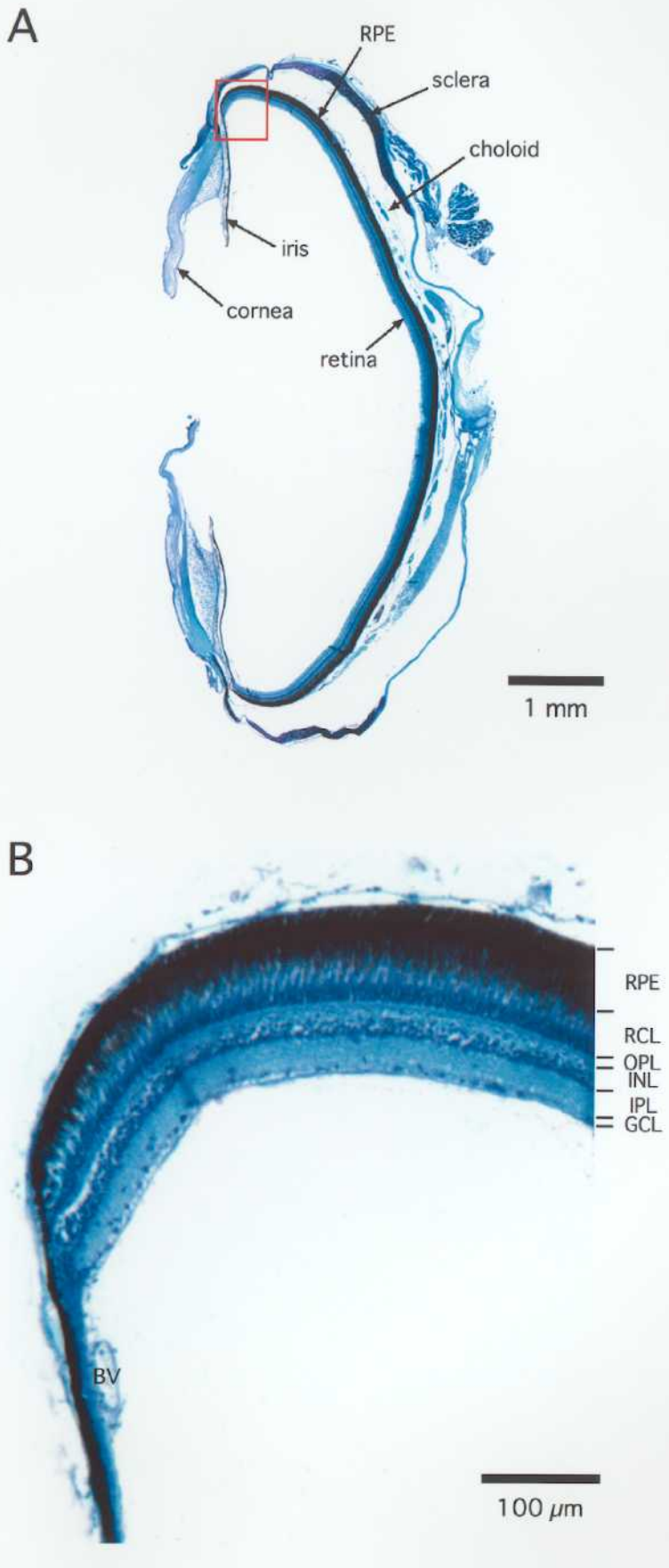
A
RPE
sclera
choloid
iris
cornea
retina
1 mm
B
RPE
RCL
OPL
INL
IPL
GCL
BV
100 μm

Figure 9. A light micrograph of the goldfish retina showing the three nuclear layers, two plexiform layers and the retinal pigmented epithelium. Paraffin section stained with toluidine blue. RPE, retinal pigmented epithelium. Other abbreviations are the same as those in Figure 2.

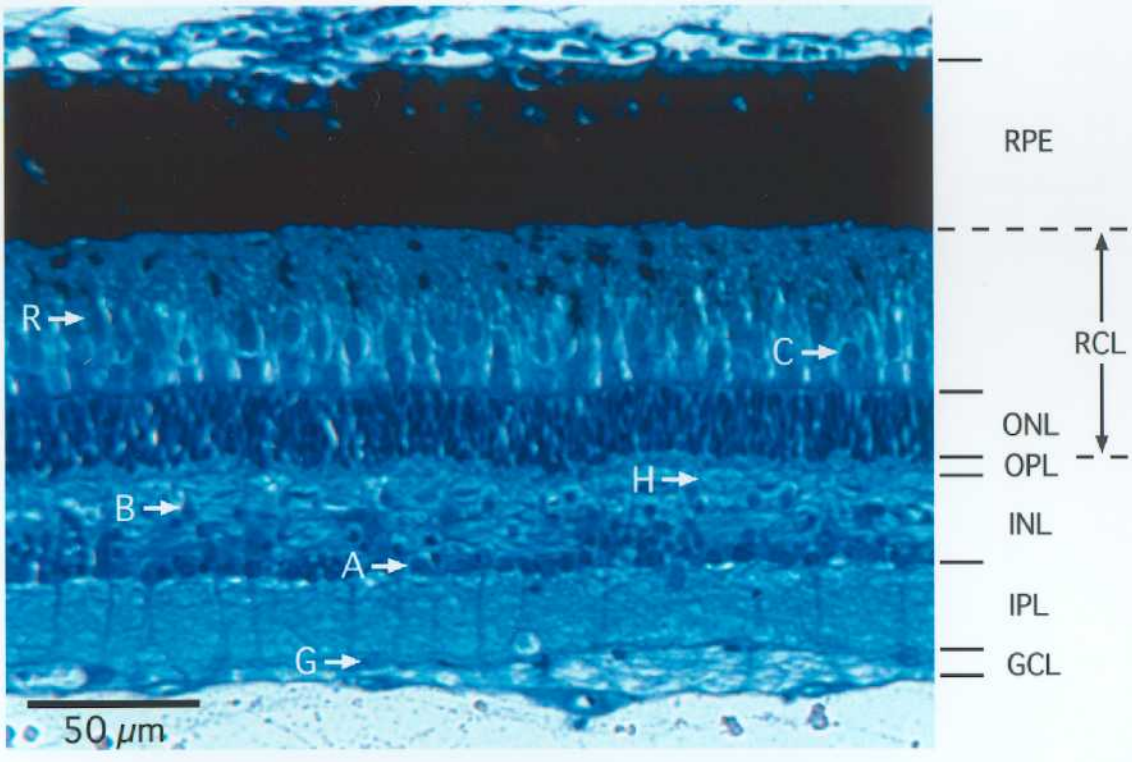
RPE
RCL
R
C
ONL
OPL
H
B
INL
A
IPL
G
GCL
50 μm

Figure 10. Transverse cryosection of goldfish peripheral retina. Arrows indicate the position of the marginal region. **A:** Light micrograph of a peripheral retina under Nomarski optics. **B:** Fluorescence micrograph of the corresponding section indicating the location of proliferating cell nuclear antigen (PCNA)-immunopositive marginal progenitor cells. RPE, retinal pigmented epithelium; M, marginal region; BV, blood vessel. Other abbreviations are the same as those in Figure 2.

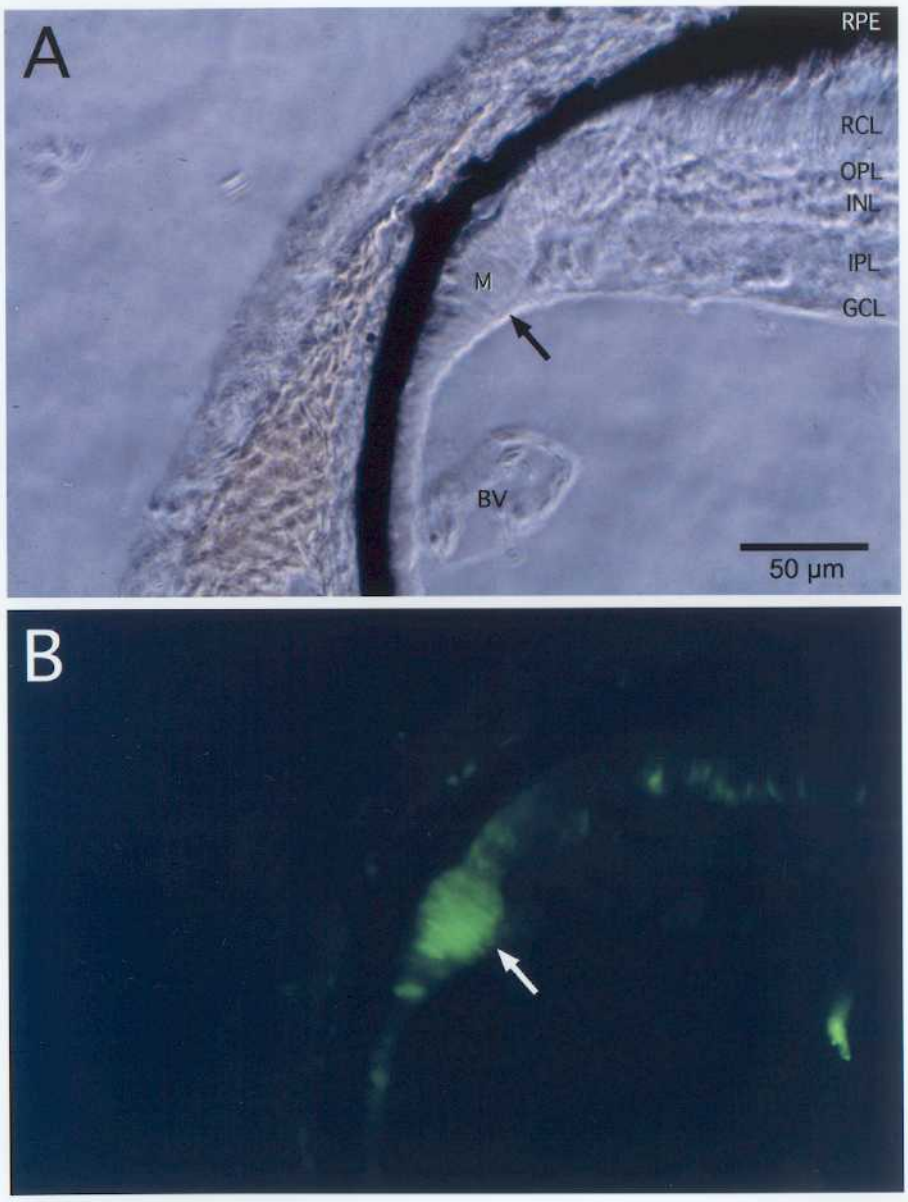
A
RPE
RCL
OPL
INL
IPL
GCL
M
BV
50 µm
B

Figure 11. Photomicrograph of a living slice preparation of peripheral retina under Nomarski optics (**A**) and scheme of the peripheral retina (**B**). The peripheral retina was broadly divided into three regions: the marginal, intermediate, and mature regions (see text). Vertical line indicates boundary between intermediate and mature regions. M, marginal region. Other abbreviations are the same as those in Figure 2. Scale bar = 30 μm.

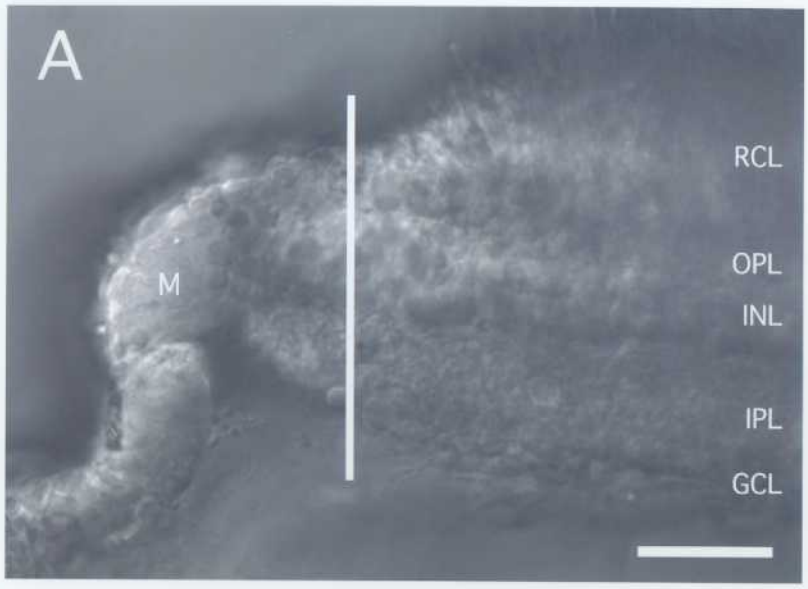
A
M
RCL
OPL
INL
IPL
GCL

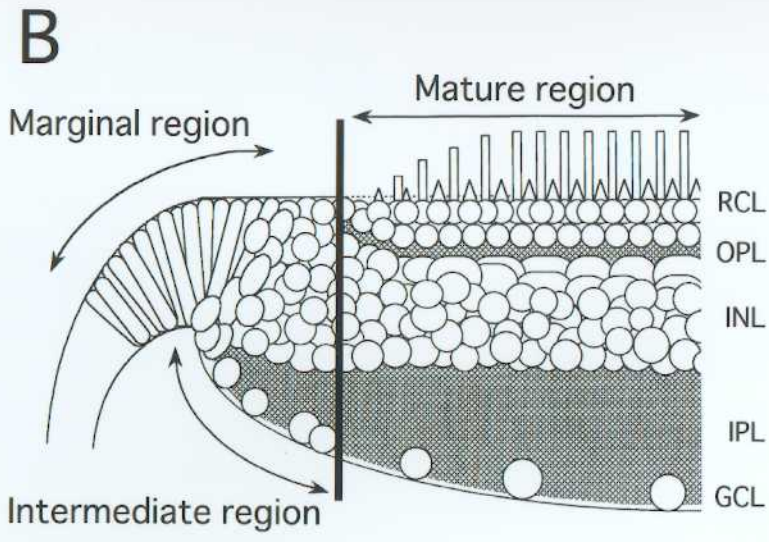
B
Mature region
Marginal region
RCL
OPL
INL
IPL
GCL
Intermediate region

Figure 12. Whole-cell currents and morphology of a marginal progenitor cell. **A:** Currents were recorded in response to step depolarizations increasing from -60 to +15 mV in 5 mV steps, from a holding potential of -80 mV, in the presence of 20 mM TEA-Cl and 5 mM 4-AP. Note that the current increased linearly in amplitude with increases in the test potential. In this experiment, capacitive and leakage currents were not subtracted. Arrowhead, 0 current. **B:** Current-voltage relationships (I-V plot) of an intact marginal cell. **C:** Marginal cell filled with LY during electrophysiological recording in A. Cell is slender and hourglass-like in shape. **D:** Drawing of the outline of the retina shown in C. The dashed line encloses the marginal region. E, electrode; M, marginal region; BV, blood vessel; F, filter paper; IPL, inner plexiform layer. Scale Bar in C = 30 μm.

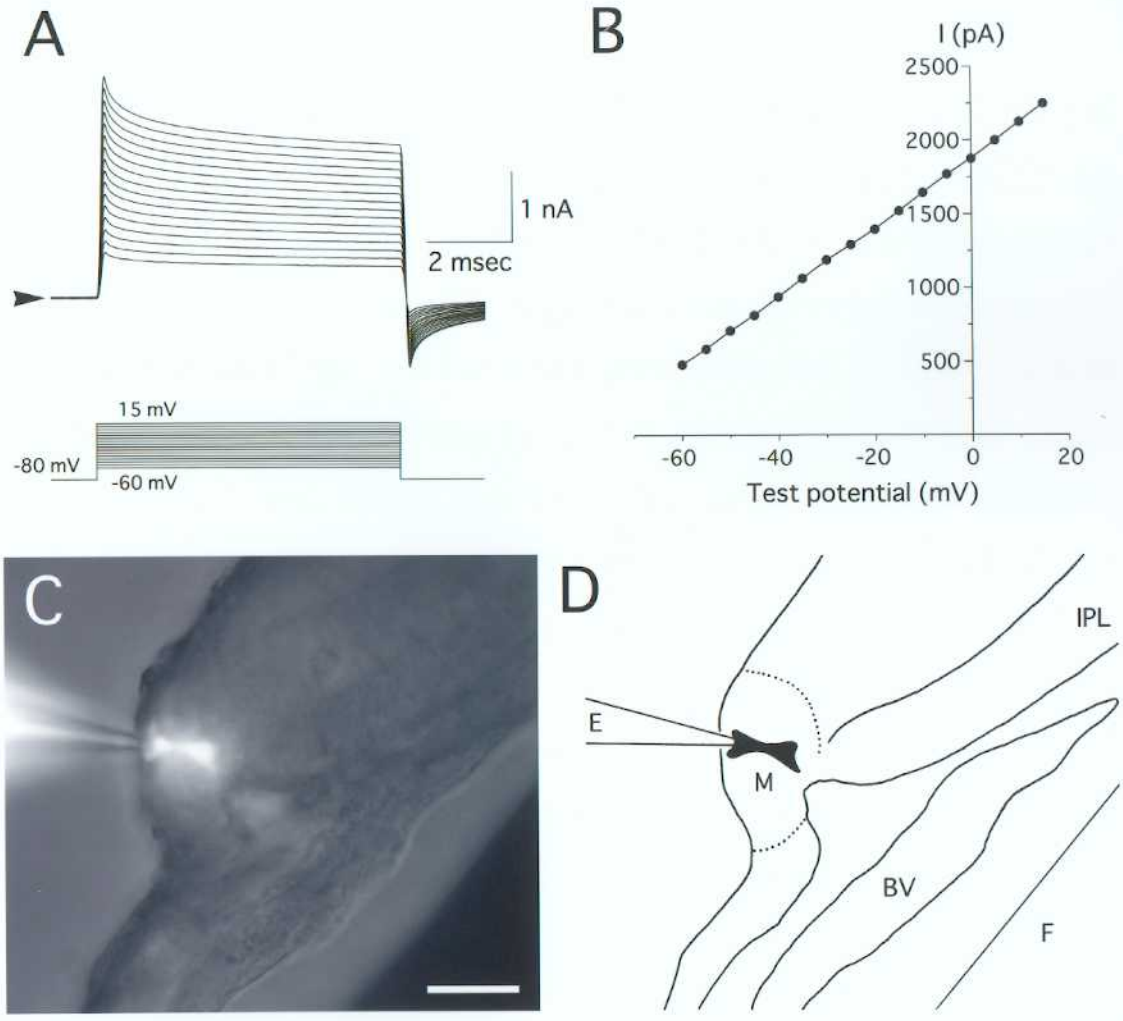
A
1 nA
2 msec
15 mV
-80 mV
-60 mV
B
I (pA)
2500
2000
1500
1000
500
-60
-40
-20
0
20
Test potential (mV)
C
D
IPL
E
M
BV
F

Figure 13. Whole-cell currents and morphology of an intermediate cell. **A:** A family of currents recorded with the same voltage-clamp protocol as that in Figure 12A. Capacitive and leakage currents were reduced by P/5 subtraction program (see Materials and Methods). **B:** Fluorescence micrograph of an LY-labeled intermediate cell. A round cell was located on the most proximal stratum of the retina. **C:** Drawing of the outline of the retina and the LY-labeled cell shown in B. The dashed line encloses the marginal region. Abbreviations are the same as those in Figure 12. Scale bar in B = 30 μm.

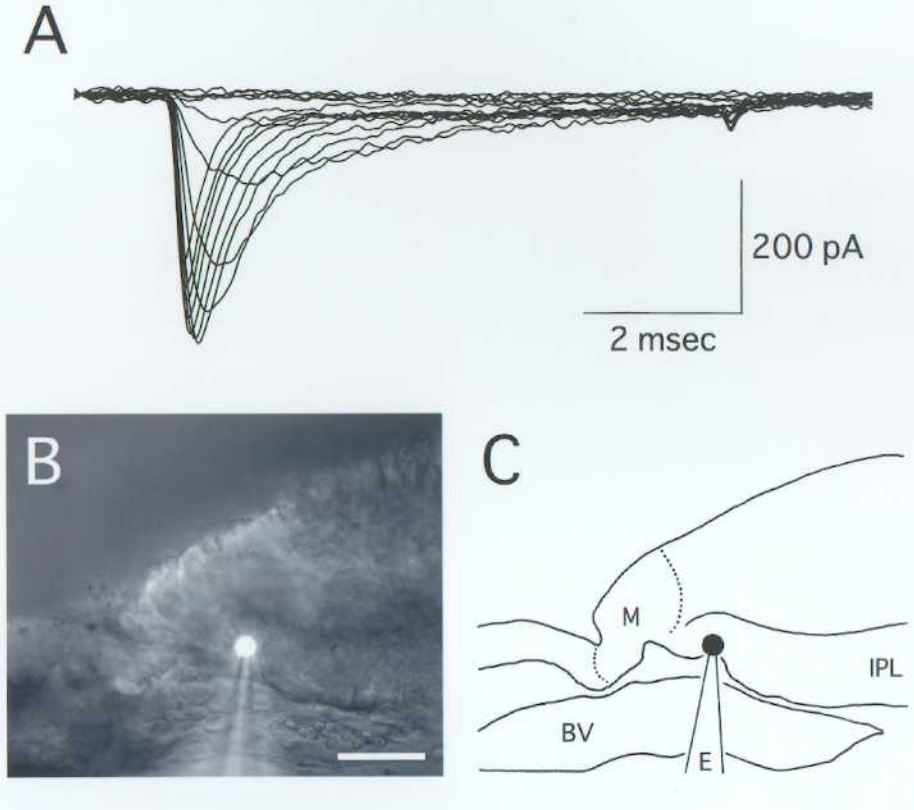
A
200 pA
2 msec
B
C
M
IPL
BV
E

Figure 14. Morphology of an intermediate cell closely apposed to the marginal region. Cell was filled with LY after recording the inward current. The same field is shown in A and B. **A:** Focus at the level of the cell body. **B:** Focus at the level of an axon-like process. **C:** Reconstruction of the LY-labeled cell shown in A and B. The dashed line encloses the marginal region. Abbreviations are the same as those in Figure 12. Scale bar in B = 30 μm.

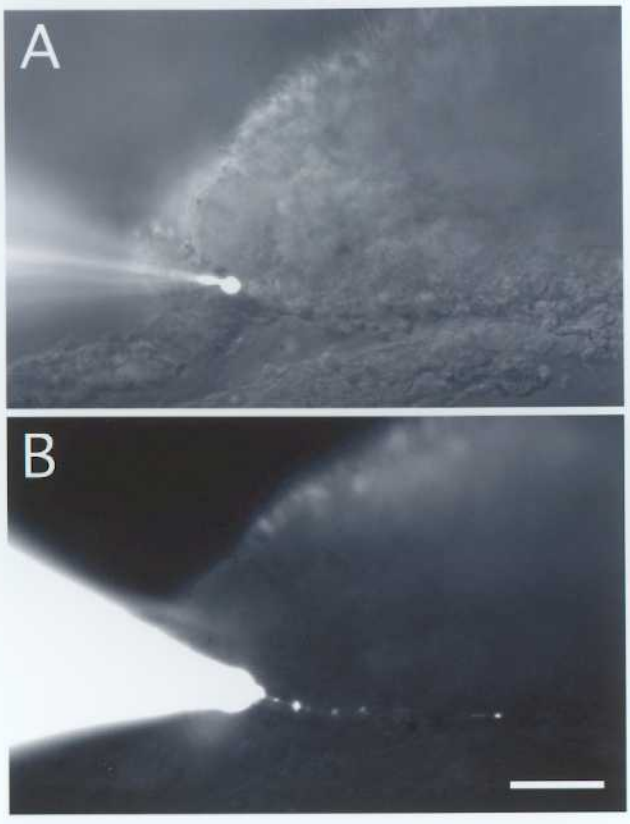
A
B
C
E
M
IPL
BV

Figure 15. Three LY-injected cells located in transition area between the intermediate and mature regions. **A:** A cell with two processes, one is extending to the marginal region (arrow) and the other along the vitreal surface (arrowhead). **B:** A cell with a process extending in the IPL without an axon-like process (arrowhead). **C:** A cell with a process extending laterally in the IPL (arrowhead). E, electrode. Each scale bar = 30 μm.

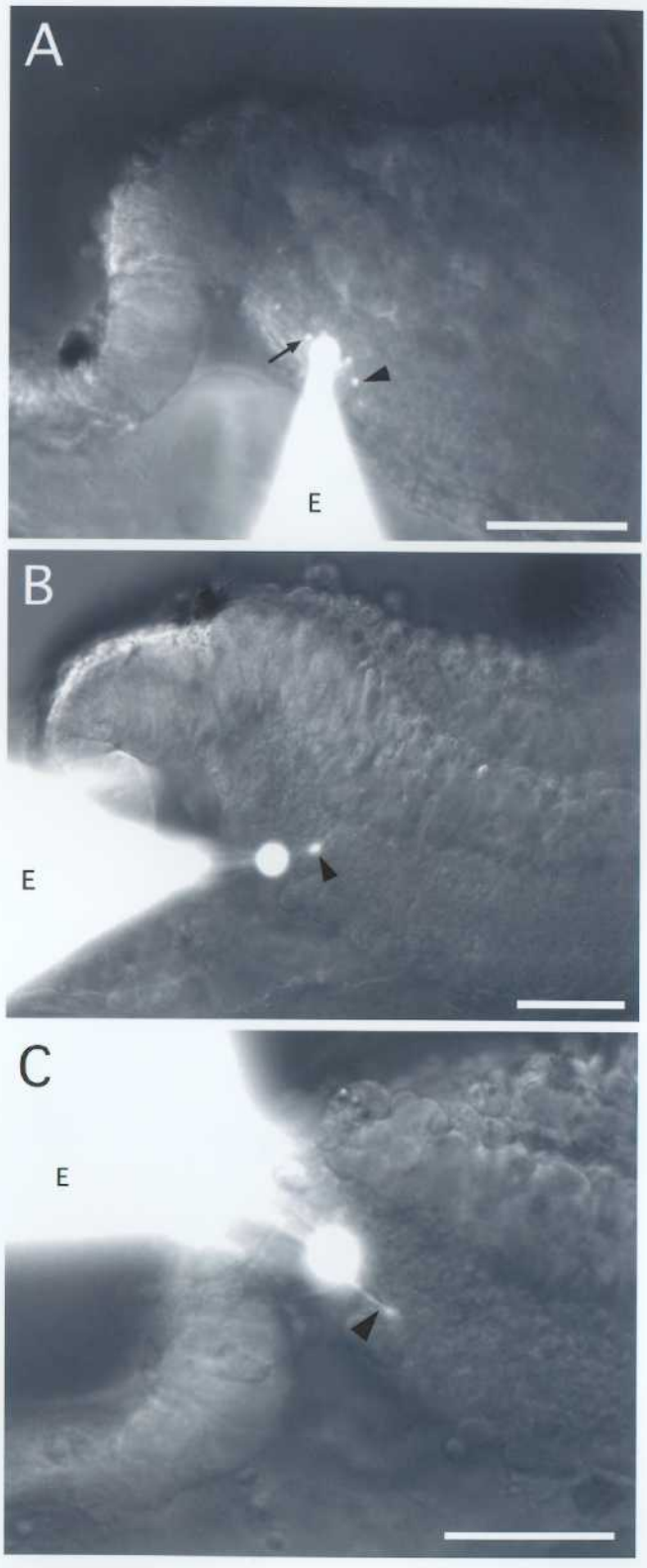
A
E
B
E
C
E

Figure 16. Block of inward currents by tetrodotoxin (TTX) in an intermediate cell. The current traces were recorded with the voltage-clamp protocol shown in Figure 12A. **A:** A family of currents recorded in control solution. **B:** A block of these currents at 2 minutes after application of 1 μM TTX. **C:** Recovery of the currents after 5 minutes of washing with TTX-free solution.

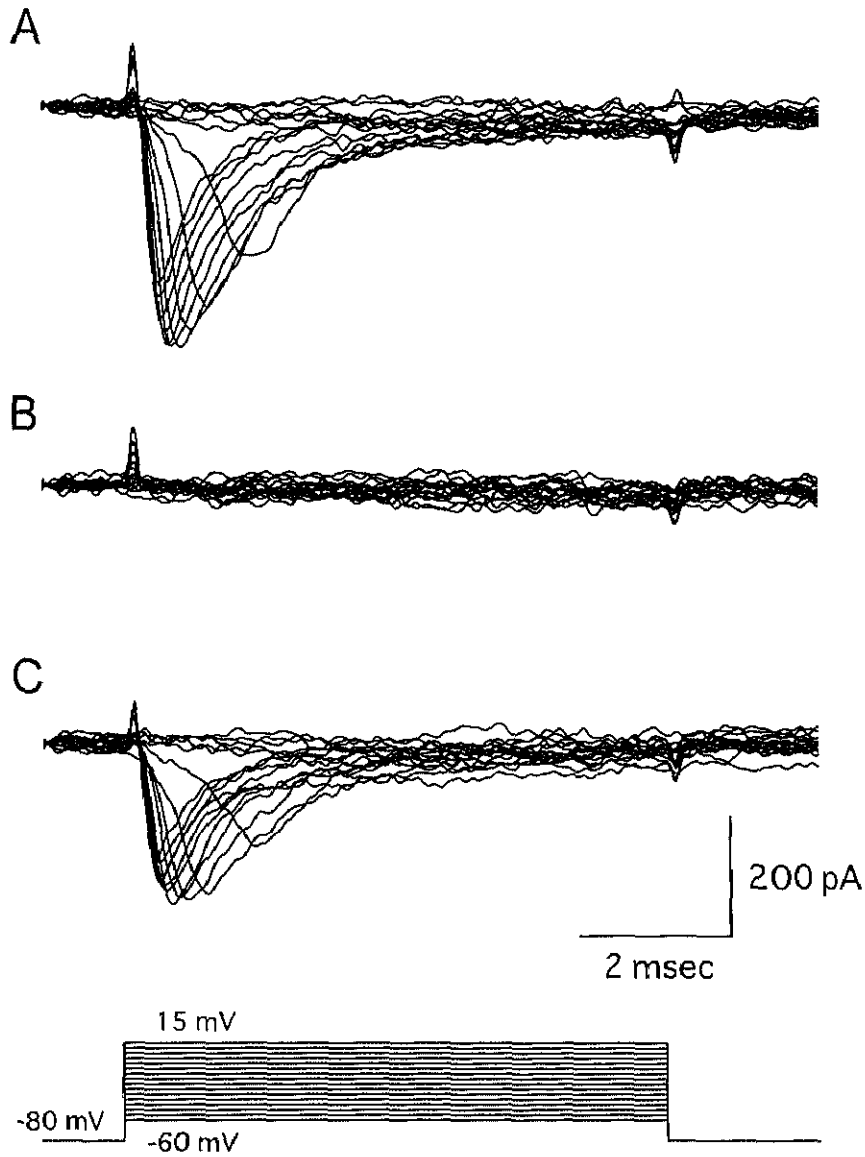
A
B
C
200 pA
2 msec
15 mV
-80 mV
-60 mV

Figure 17. Current-voltage relations of the inward current in intermediate and mature ganglion cells. Error bars plot the mean ± SE of the current peak from 17 intermediate cells (circles) and 10 mature ganglion cells (squares).

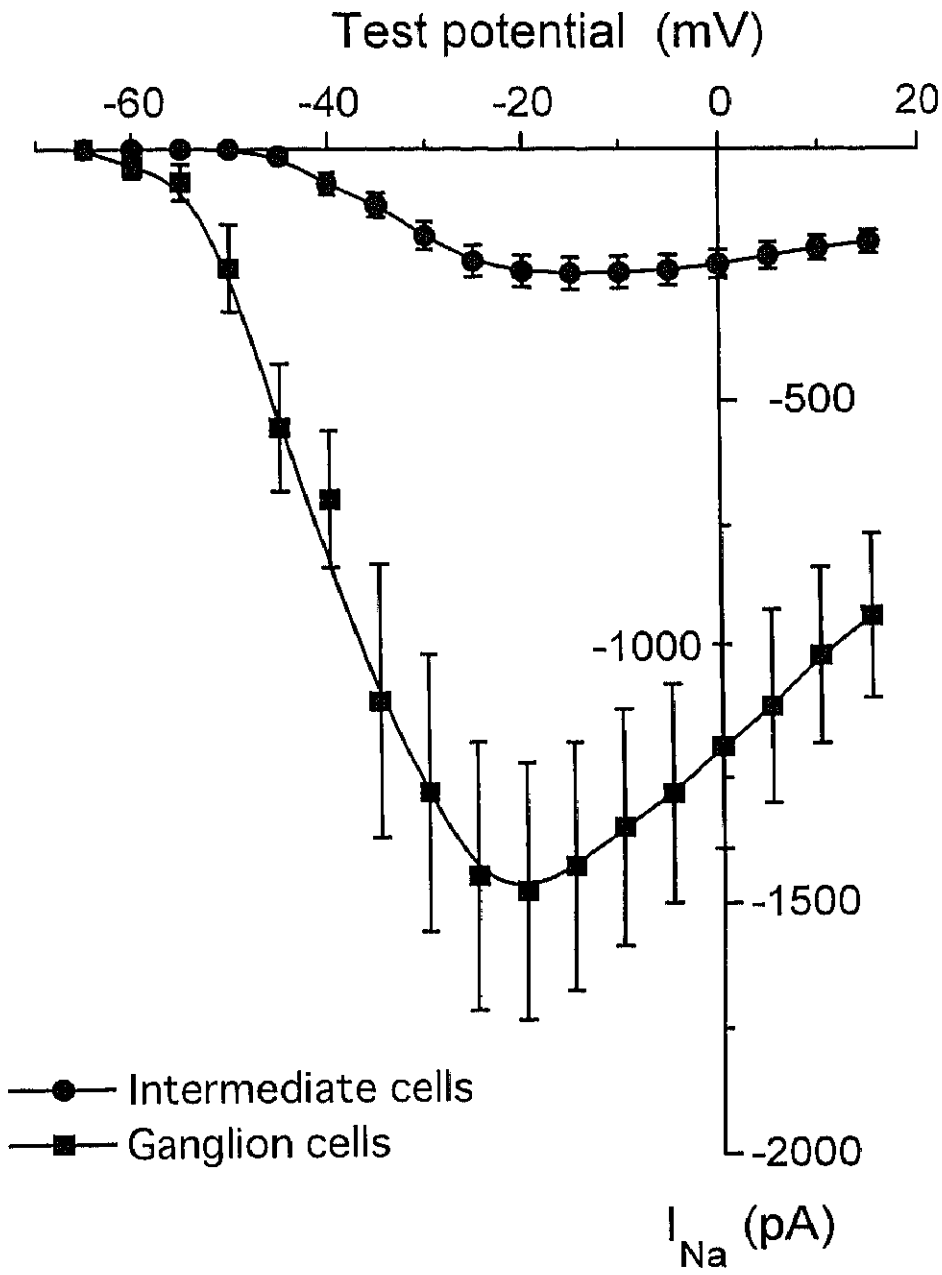
Test potential (mV)
-60
-40
-20
0
20
-500
-1000
-1500
-2000
Intermediate cells
Ganglion cells
I_{Na} (pA)

Figure 18. Whole-cell currents and morphology of a cell located in the distal level of the intermediate region. **A:** Currents were recorded in response to step depolarizations increasing from -60 to +15 mV in 5 mV steps, from a holding potential of -80 mV, in the presence of 20 mM extracellular TEA-Cl and 5 mM 4-AP. No Na^+ currents were detected. Capacitive and leakage currents were reduced by P/5 subtraction program (see Materials and Methods). **B:** Intermediate cell filled with LY during electrophysiological recording in A. Focus at the level of the cell body. **C:** Intermediate cell same as that in B, but focused at the level of a long branching process. **D:** Reconstruction of the LY-labeled cell shown in B and C, and drawing of the outline of the peripheral retina. The dashed line encloses the marginal region. Abbreviations are the same as those in Figure 12. Scale bar in C = 30 μm.

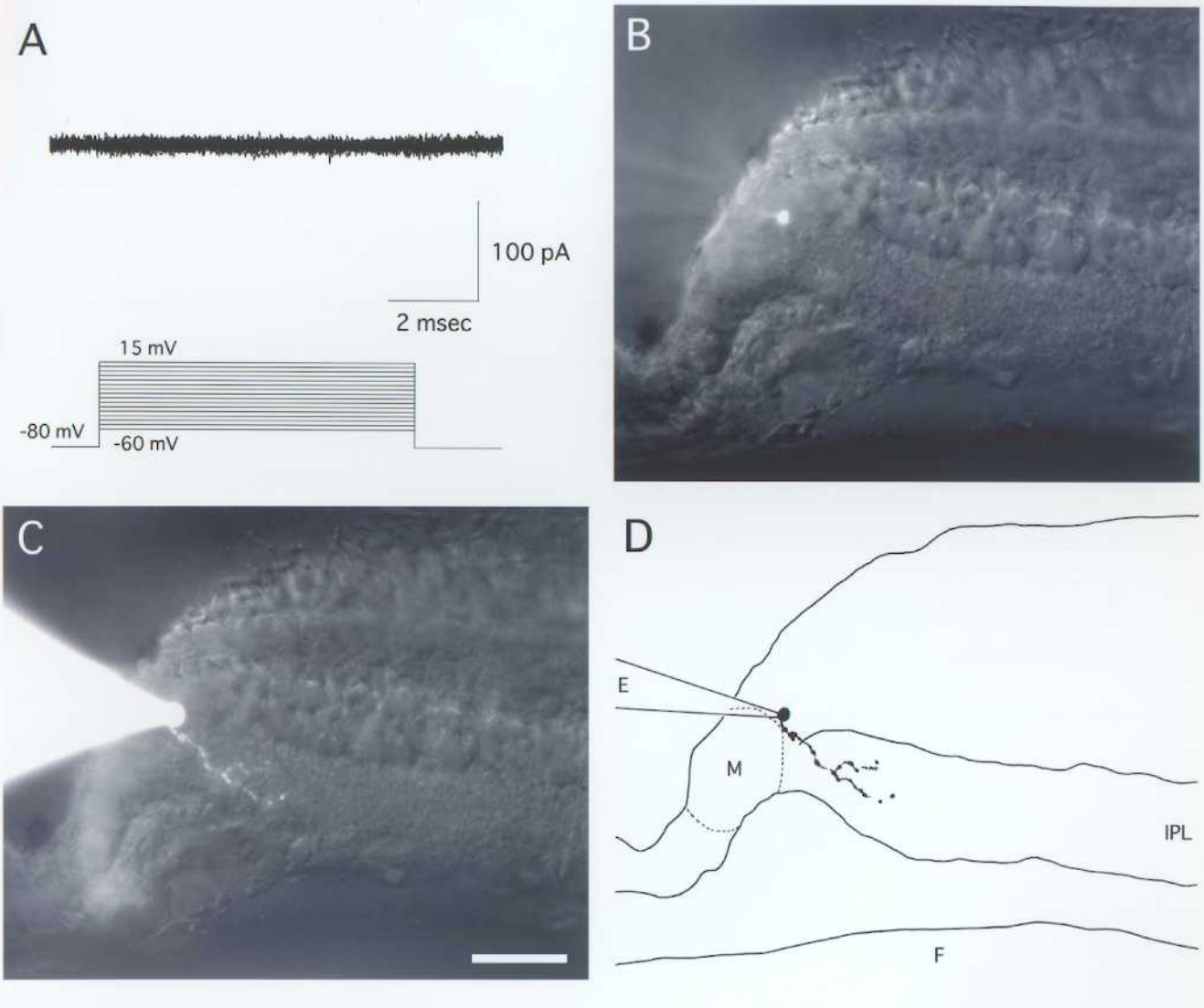
A
100 pA
2 msec
15 mV
-80 mV
-60 mV
B
C
D
E
M
IPL
F

Figure 19. Inward currents in a mature ganglion cell and location of the same cell in slice preparation. **A:** Currents recorded with the voltage-clamp protocol shown in Figure 13. The currents activated by larger depolarizations display a transient component, followed by a persistent component. Both current components were blocked by tetrodotoxin (TTX). **B:** Mature retinal ganglion cell filled with LY during recording in A and viewed under a combination of epifluorescence and incandescent illumination. The round cell soma was located at the most proximal stratum of the retina. **Inset** shows the same cell at higher magnification. Arrow points to axon-like protrusion. Abbreviations are the same as those in Figure 2. Scale bar = 30 μm.

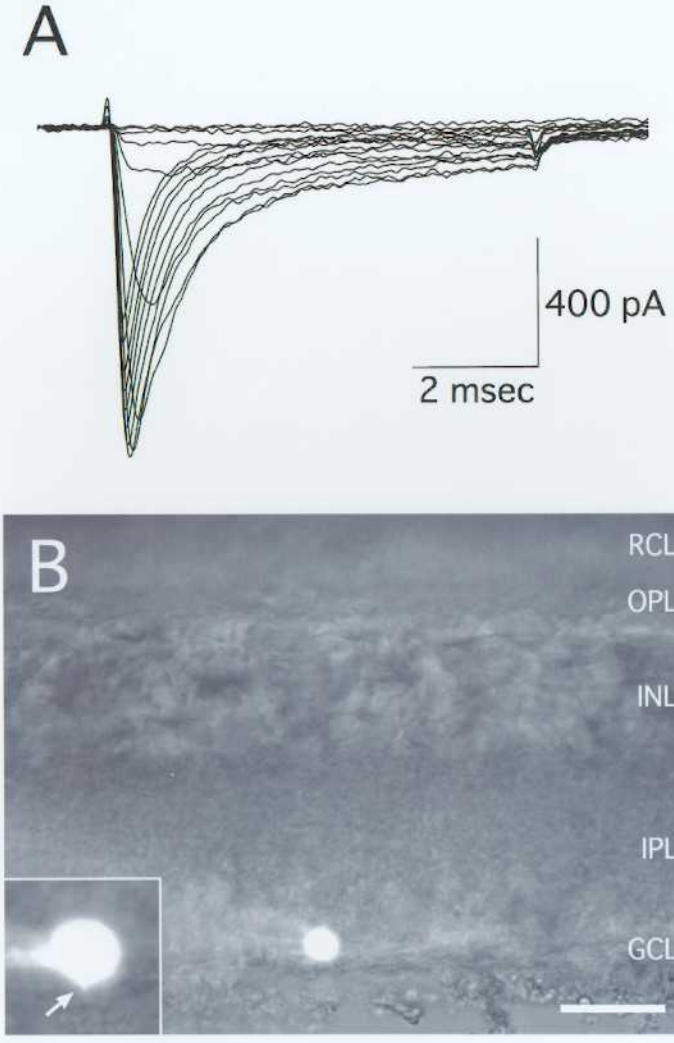
A
400 pA
2 msec
B
RCL
OPL
INL
IPL
GCL

Figure 20. Fluorescence micrograph of two morphological types of mature ganglion cells identified by LY. **A:** A montage photomicrograph showing a cell that has an axon (arrows) and a dendritic process in the proximal part of the IPL (arrowhead). **B:** A cell has an axon (arrow) and a dendritic process into the distal part of the IPL (arrowhead). E, electrode. Other abbreviations are the same as those in Figure 2. Scale bar = 30 μm.

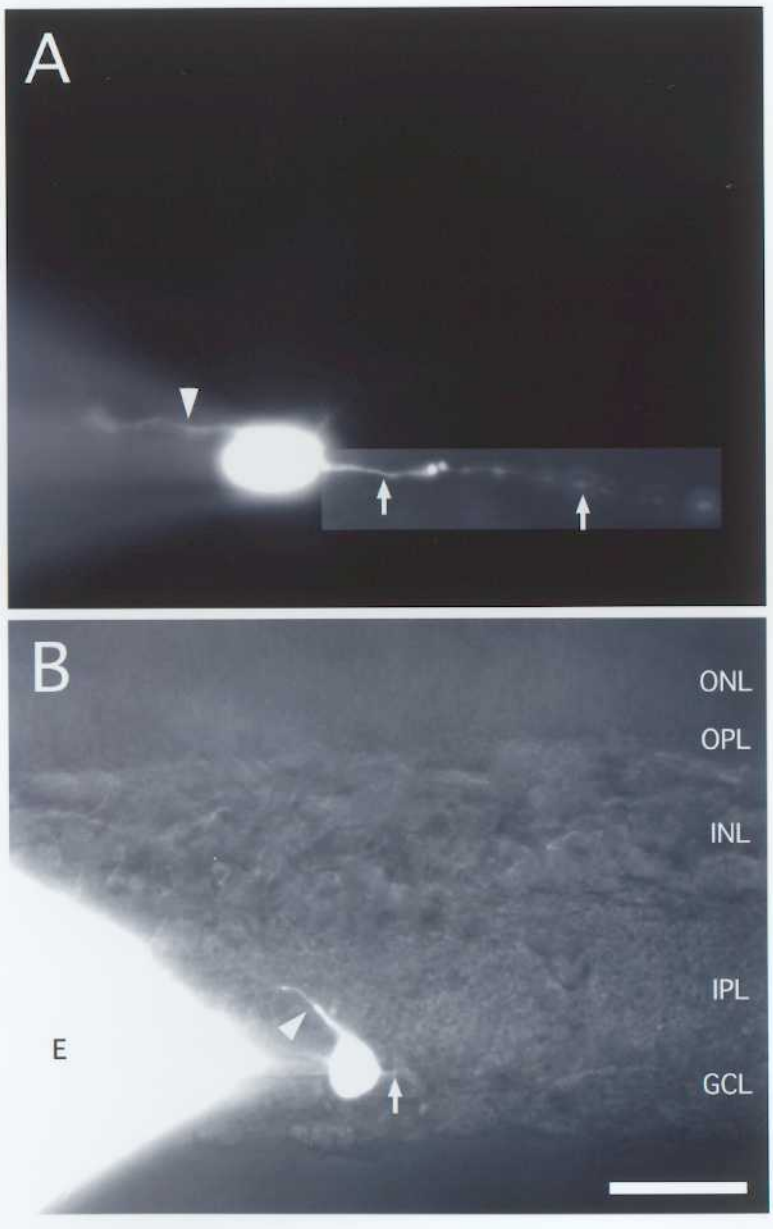
A
B
ONL
OPL
INL
IPL
GCL
E

Figure 21. Whole cell currents of a progenitor cell in retinal margin. **A:** Cell was initially voltage-clamped at a resting potential of -35 mV and then the membrane potential was stepped from -195 to +125 mV in 40 mV increments (inset). Each test voltage step of 350 msec duration was applied every 3 sec. Currents were recorded under suppression of K^+ and Ca^{2+} currents. **B:** Steady state current (I_{ss}) amplitude measured at 345 msec was plotted against the test voltage (V).

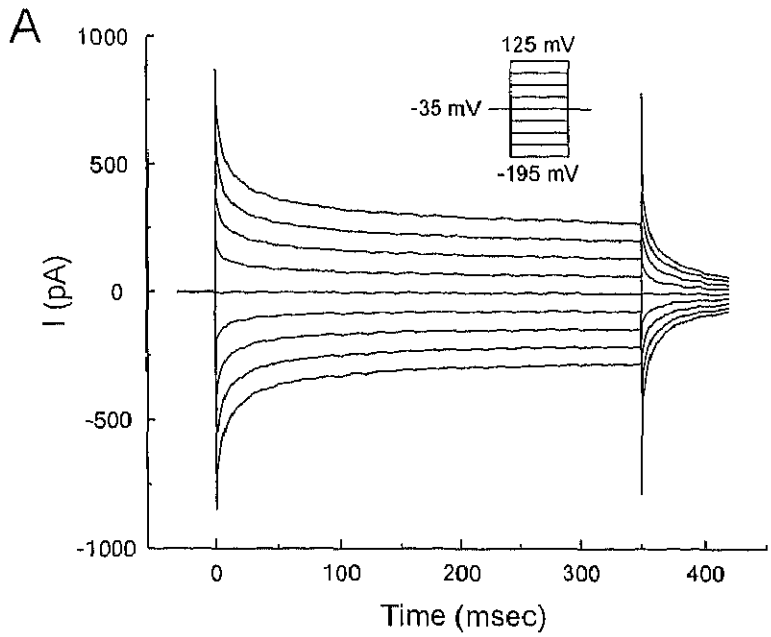
A
1000
500
0
-500
-1000
I (pA)
125 mV
-35 mV
-195 mV
0
100
200
300
400
Time (msec)

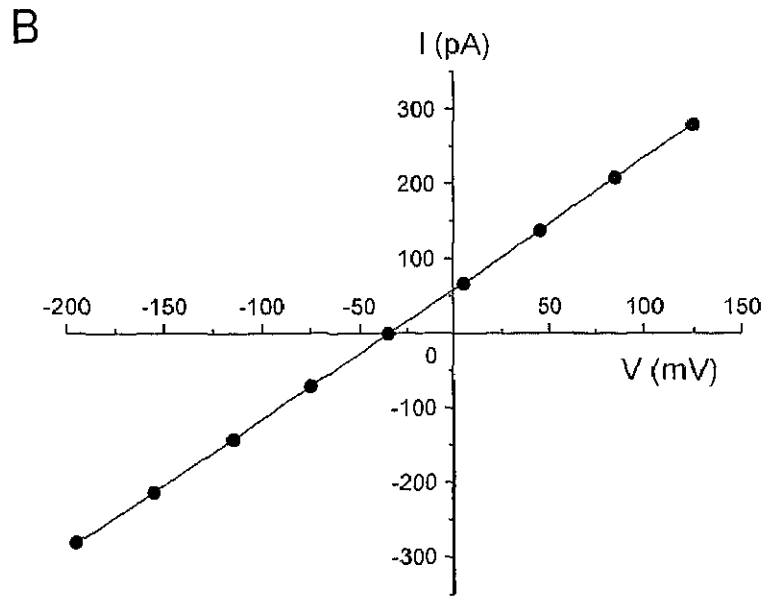
B
I (pA)
300
200
100
-200
-150
-100
-50
50
100
150
0
V (mV)
-100
-200
-300

Figure 22. Time- and voltage-dependent decline of whole-cell currents of a progenitor cell. **A:** Cell was initially voltage-clamped at a resting potential of -18 mV and then the membrane potential was stepped from -168 to +132 mV in 30 mV increments (inset). Currents were recorded under suppression of K^+ and Ca^{2+} currents. Symmetrical form of voltage-dependent current decay was observed. **B:** The current-voltage relationships obtained from a family of currents in A. The instantaneous (I_{inst}) and steady state (I_{ss}) currents, measured at 20 msec (open circles) and 345 msec (closed circles) of each pulse, were plotted against the test voltage (V).

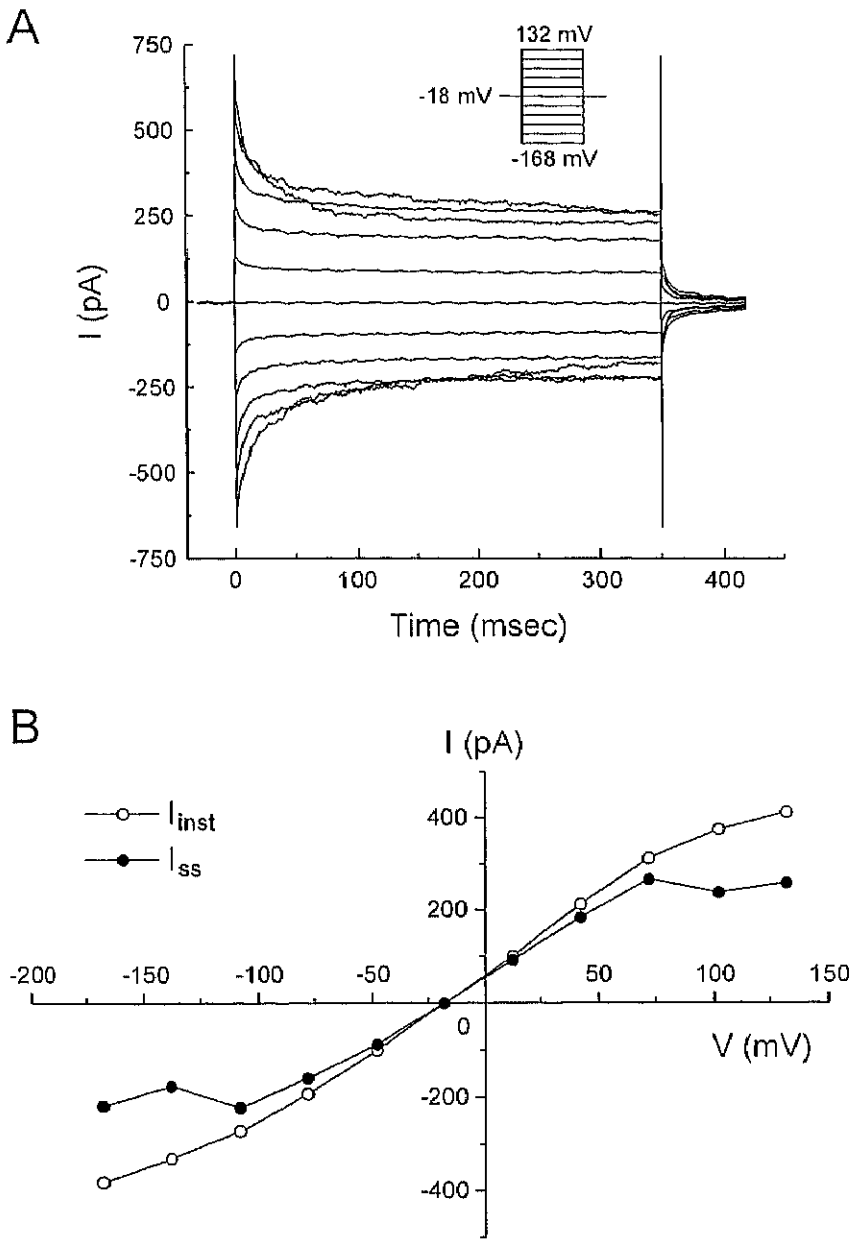
A
132 mV
-18 mV
-168 mV
750
500
250
0
-250
-500
-750
I (pA)
0
100
200
300
400
Time (msec)
B
I (pA)
I_{inst}
I_{ss}
400
200
-200
-400
-200
-150
-100
-50
50
100
150
0
V (mV)

Figure 23. Photomicrograph of an LY-labeled cell and tracer coupling with its neighbors. A cell examined electrophysiologically in Figure 21 was identified by injection of both LY and biocytin. **A:** Fluorescence micrograph of an LY-labeled cell (arrow). Peripheral retina was visualized under a combination of epifluorescence and incandescent lights. **B:** Light micrograph of tracer-coupled cells (arrow). Tracer coupling was only restricted in marginal region. BV, blood vessel; F, filter paper. Other abbreviations are the same as those in Figure 2. Scale bar = 30 μm.

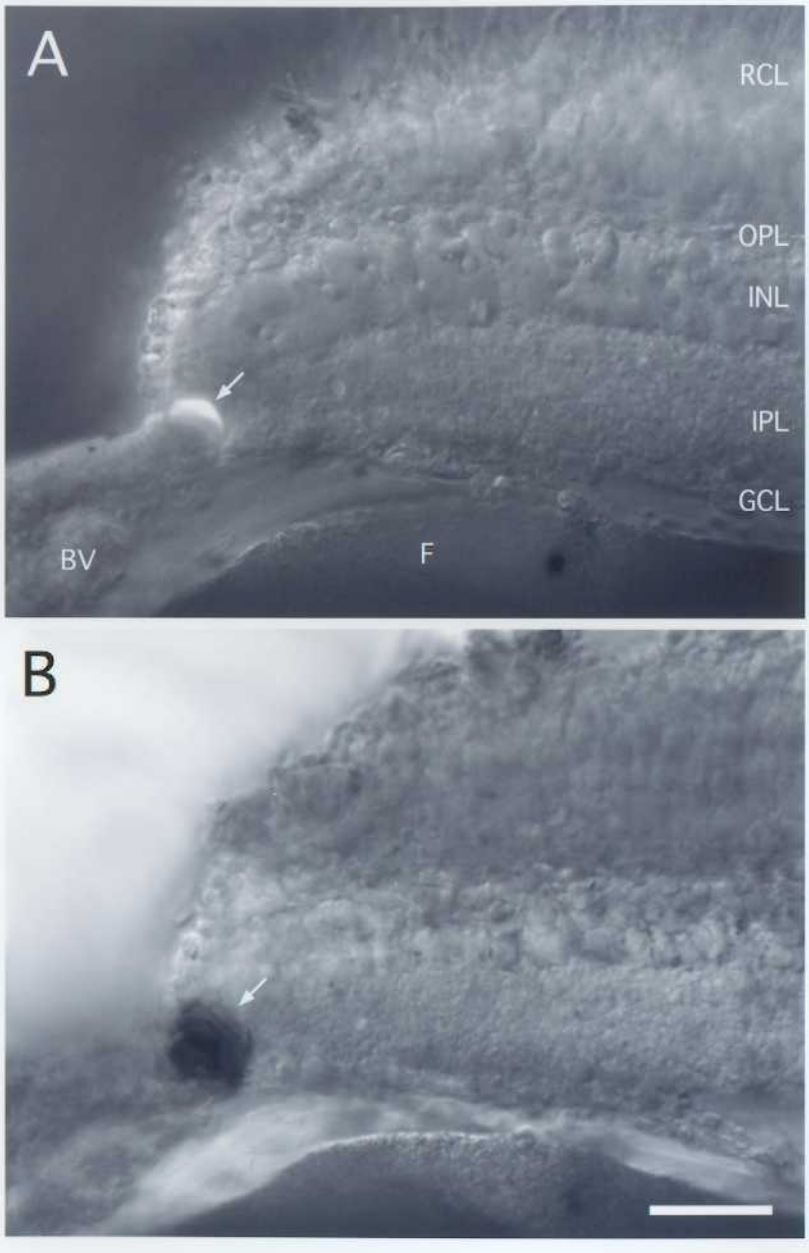
A
RCL
OPL
INL
IPL
GCL
BV
F
B

Figure 24. Whole-cell currents and morphology of a mechanical isolated marginal progenitor cell. **A:** Small currents were recorded in response to step depolarizations increasing from -60 to +15 mV in 5 mV steps, from a holding potential of -80 mV (inset), in the presence of extracellular 20 mM TEA-Cl and 5 mM 4-AP. **B:** The current-voltage relationships of the isolated marginal cell shown in A. A slope conductance estimated from the slope of the line was 0.28 nS. **C:** Intermediate cell filled with LY during electrophysiological recording in A. Cell was round-shaped. **D:** Drawing of the outline of the peripheral retina and LY-labeled cell shown in C. The dashed line encloses the marginal region. Abbreviations are the same as those in Figure 12. Scale bar in C = 30 μm.

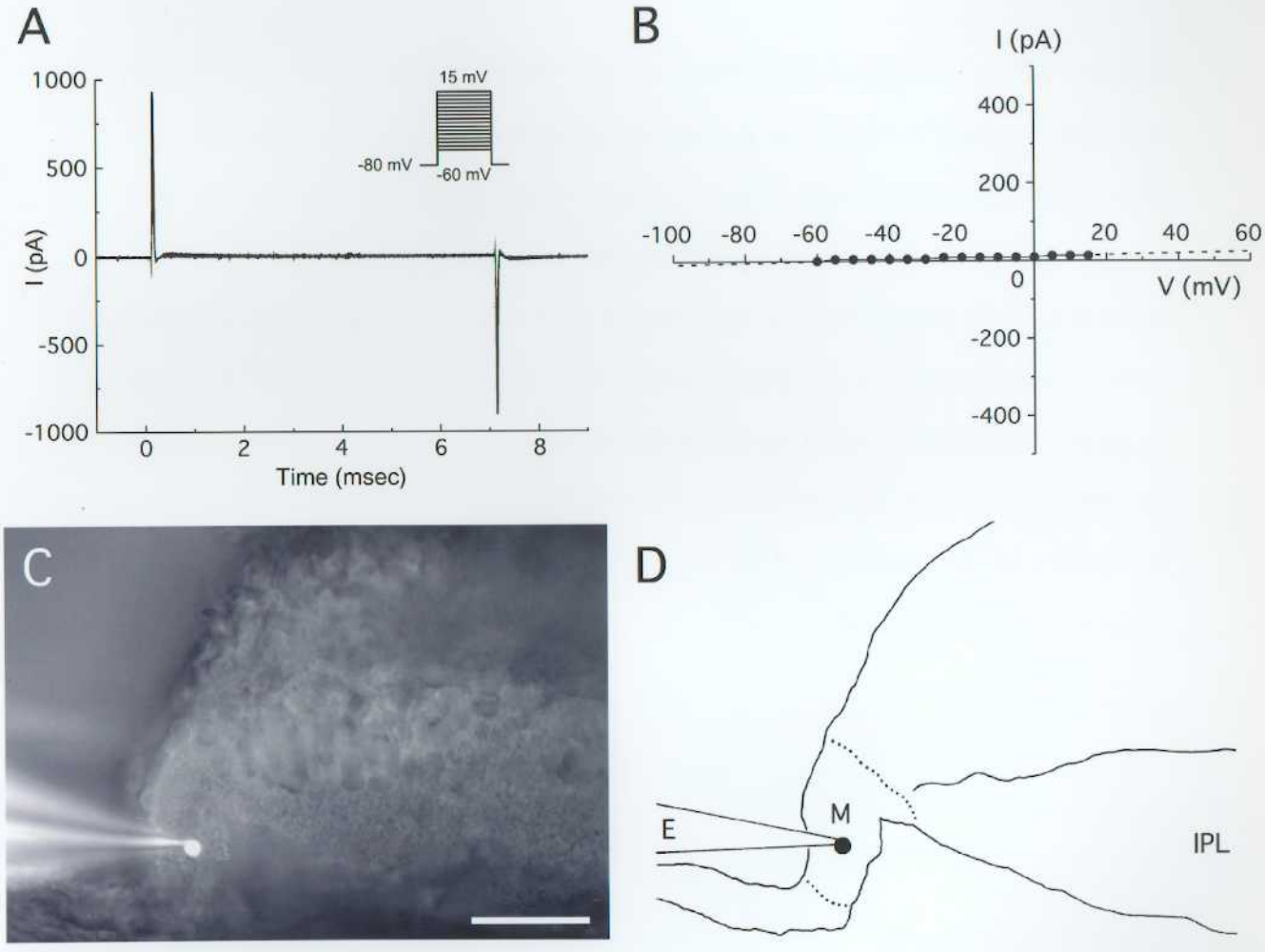
A
1000
500
0
-500
-1000
I (pA)
0
2
4
6
8
Time (msec)
15 mV
-80 mV
-60 mV
B
I (pA)
400
200
-100
-80
-60
-40
-20
20
40
60
0
V (mV)
-200
-400
C
D
E
M
IPL

Figure 25. Effects of halothane on the whole-cell currents. Cell was initially voltage-clamped at a resting potential of -22 mV and then the membrane potential was stepped from -182 to +138 mV in 20 mV increments. Currents were recorded under suppression of K^+ and Ca^{2+} currents. Each set of records consists of five superimposed current traces sampled from a series of voltage steps. The voltage is written to the right in C. **A:** A family of currents recorded in the control solution. **B:** A block of the currents at 2 minutes after application of 5 mM halothane. **C:** Recovery of the currents after 5 minutes of washing with halothane-free solution. Arrowhead, 0 current.

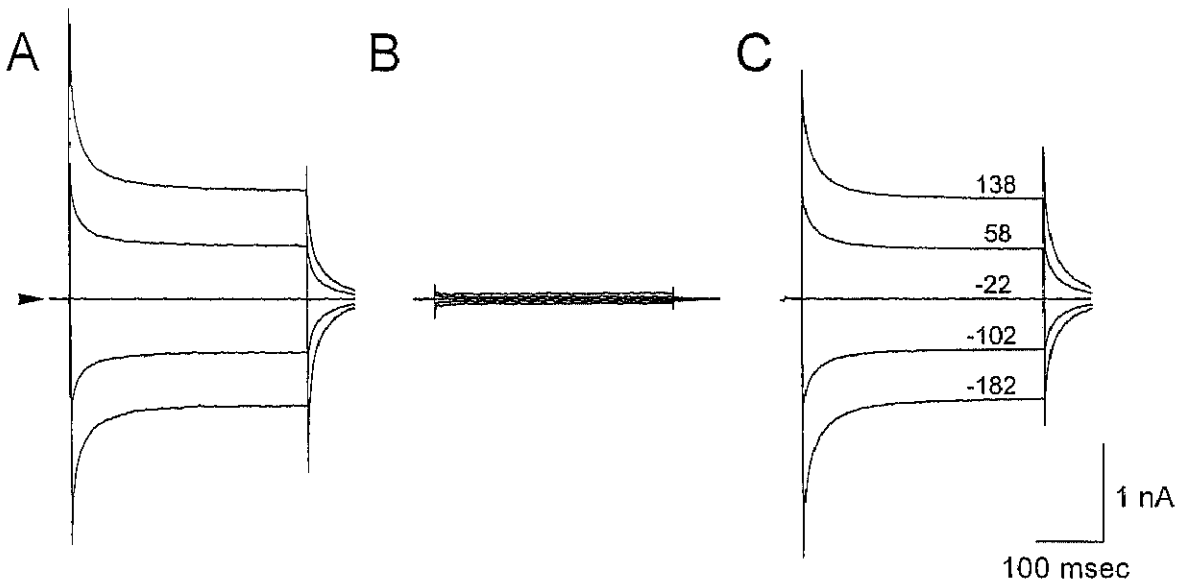
A
B
C
138
58
-22
-102
-182
1 nA
100 msec

Figure 26. Effects of extracellular pH on currents recorded from a progenitor cell. Cell was voltage-clamped to a resting potential of -24 mV, and then the membrane potential was stepped from -184 to +136 mV in 20 mV increments. Each set of records consists of five superimposed current traces sampled from a series of voltage steps. The voltage is written to the right in C. **A:** pH 6.4. **B:** pH 7.4. **C:** pH 8.4. Arrowhead, 0 current.

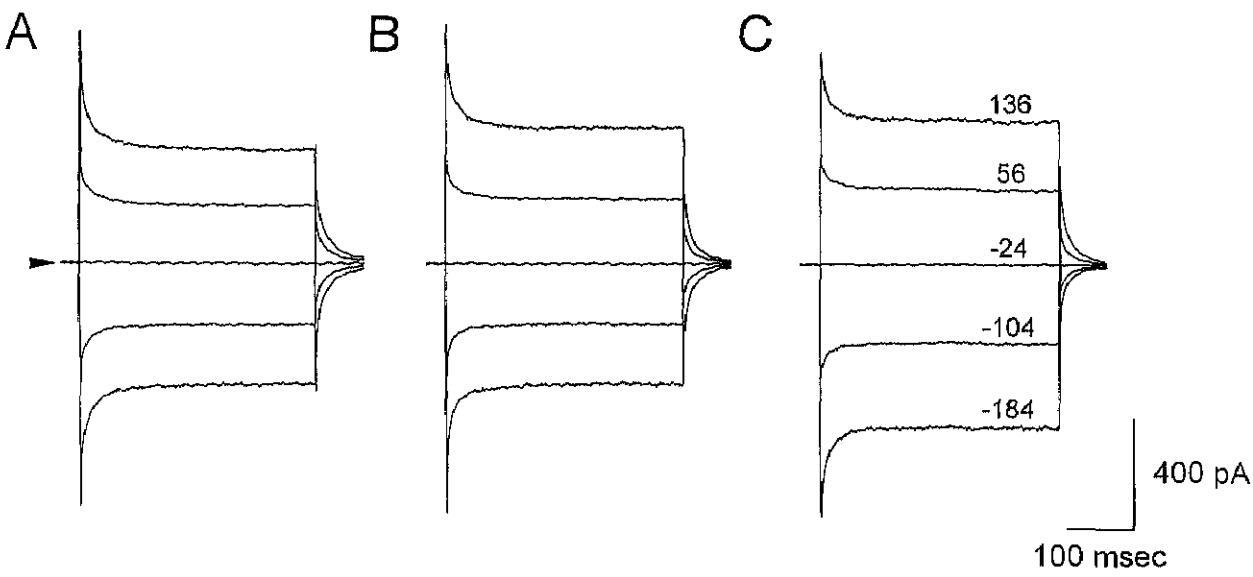
A
B
C
136
56
-24
-104
-184
400 pA
100 msec

Figure 27. Effects of extracellular pH on voltage- and time-dependent components of gap junctional currents recorded from a progenitor cell. Cell was voltage-clamped to a resting potential of -29 mV, and then the membrane potential was stepped from -189 to +131 mV in 40 mV increments. **A:** pH 6.4. **B:** pH 7.4. **C:** pH 8.4. **D:** Current-voltage relationships measured at 50 msec of each pH shown in A, B and C. Note that voltage dependent decline in current reduced with increasing in the pH. A degree of decline was increased as pH drop. Arrowhead, 0 current.

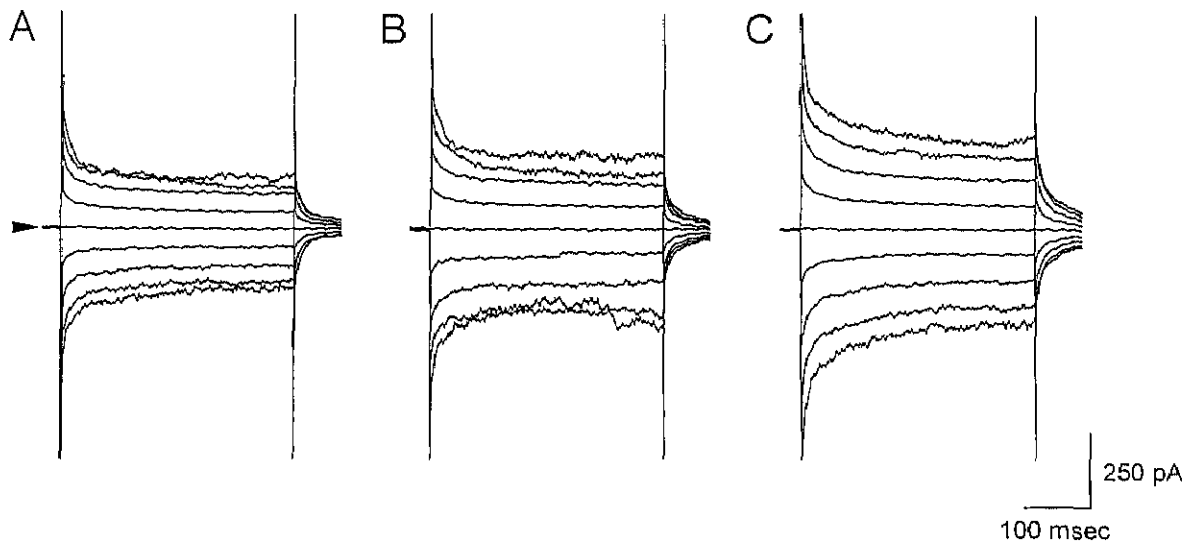
A
B
C
250 pA
100 msec

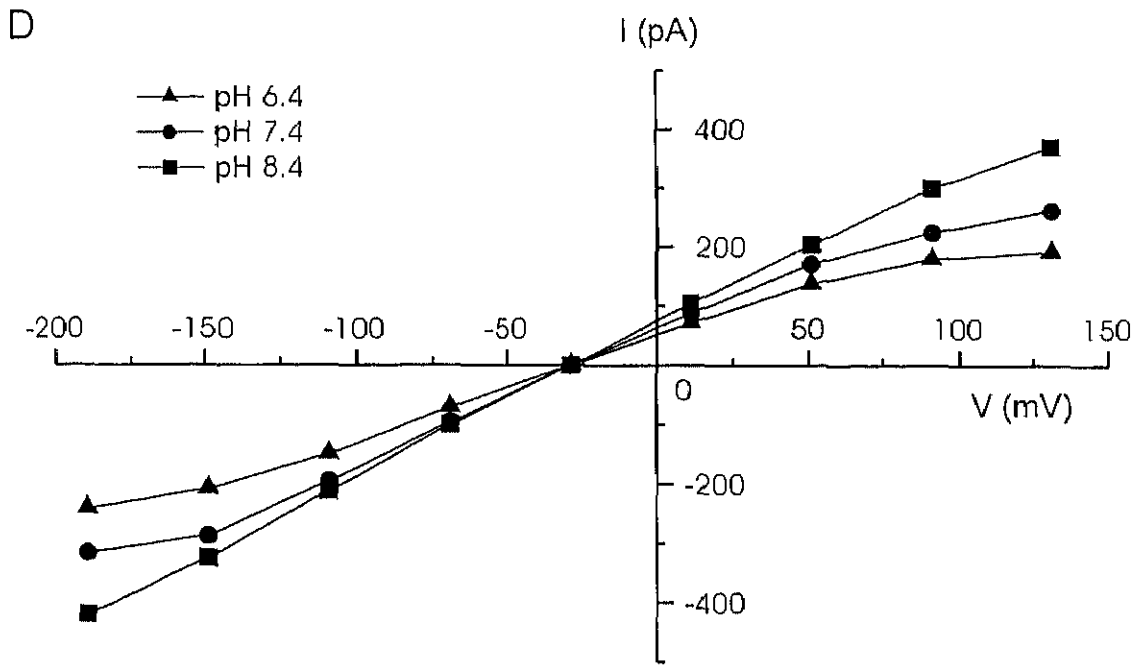
D
I (pA)
pH 6.4
pH 7.4
pH 8.4
400
200
-200
-400
-200
-150
-100
-50
50
100
150
0
V (mV)

Figure 28. Effects of dopamine (A and B) and retinoic acid (C and D) on the whole-cell currents. Cells were initially voltage-clamped at a resting potential (-20 mV) and then the membrane potentials were stepped to test voltages between -180 and +140 mV in 20 mV increments. Each set of records consists of five superimposed current traces sampled from a series of voltage steps. The voltage is written to the right in B and D, respectively. **A:** A family of currents recorded in the control solution. **B:** Current traces 3 minutes after application of 100 μM dopamine. **C:** A family of currents recorded in the control solution. **D:** Current traces 3 minutes after application of 300 μM retinoic acid. Arrowhead, 0 current.

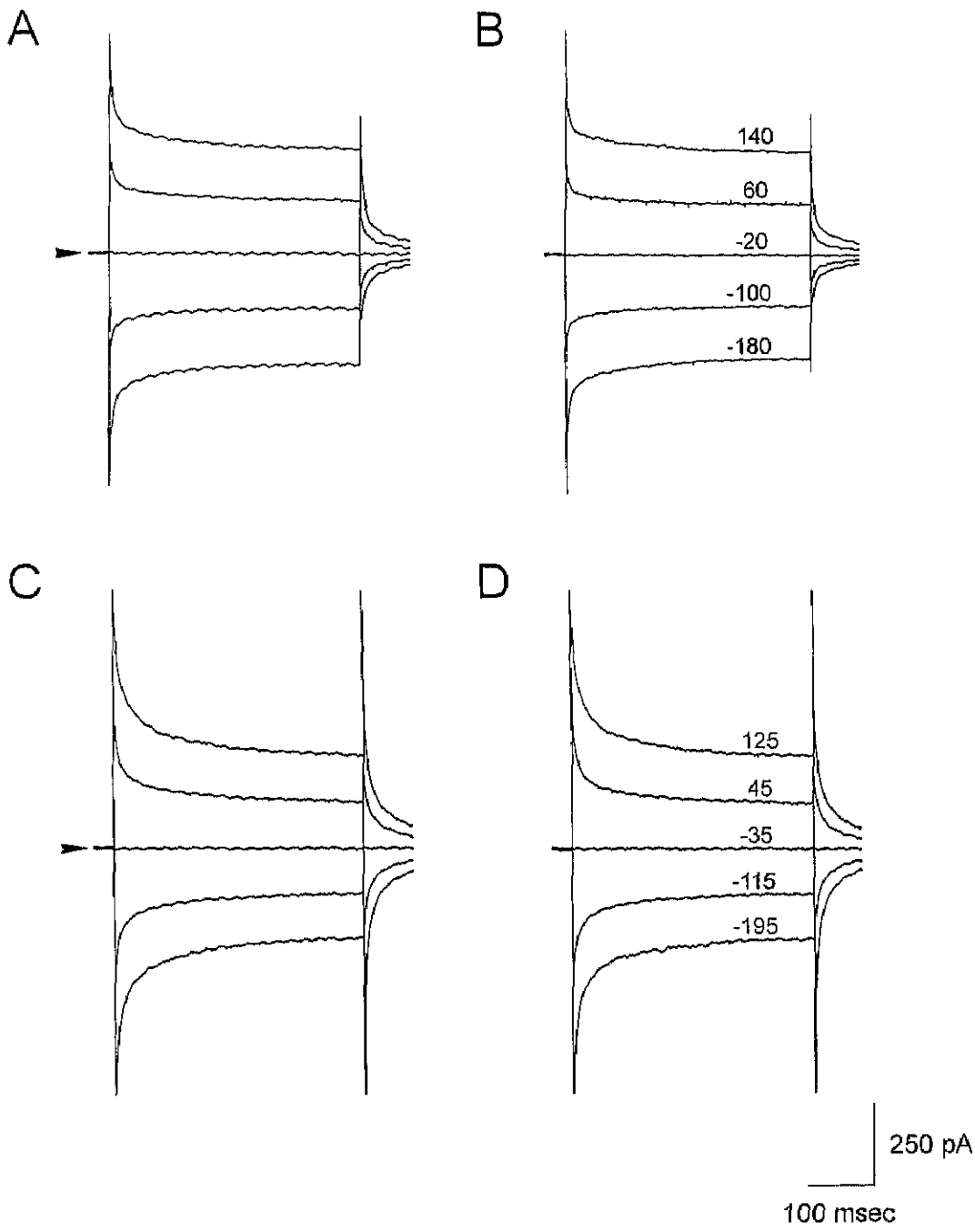
A
B
140
60
-20
-100
-180
C
D
125
45
-35
-115
-195
250 pA
100 msec

Figure 29. Whole cell currents and morphology of a cell near the retinal margin. Cell was initially voltage-clamped at a holding potential of -80 mV and then the membrane potential was stepped from -60 to +15 mV in 5 mV increments. Inward Na^+ currents were recorded under suppression of K^+ and Ca^{2+} currents. Capacitive and leakage currents were reduced by P/5 subtraction program (see Materials and Methods). The cell was injected with both LY and biocytin after current recordings. **A:** Fluorescence micrograph of an LY-labeled cell (arrow). **B:** Light micrograph of a biocytin-labeled cell (arrow). No tracer coupling was observed. **C:** Drawing of the outline of the peripheral retina including the labeled cell shown in B. The dashed line encloses the marginal region. **D:** Three superimposed current traces sampled from a series of voltage steps. The voltage is written to each trace. Abbreviations are the same as those in Figure 12. Scale bar in B = 30 μm.

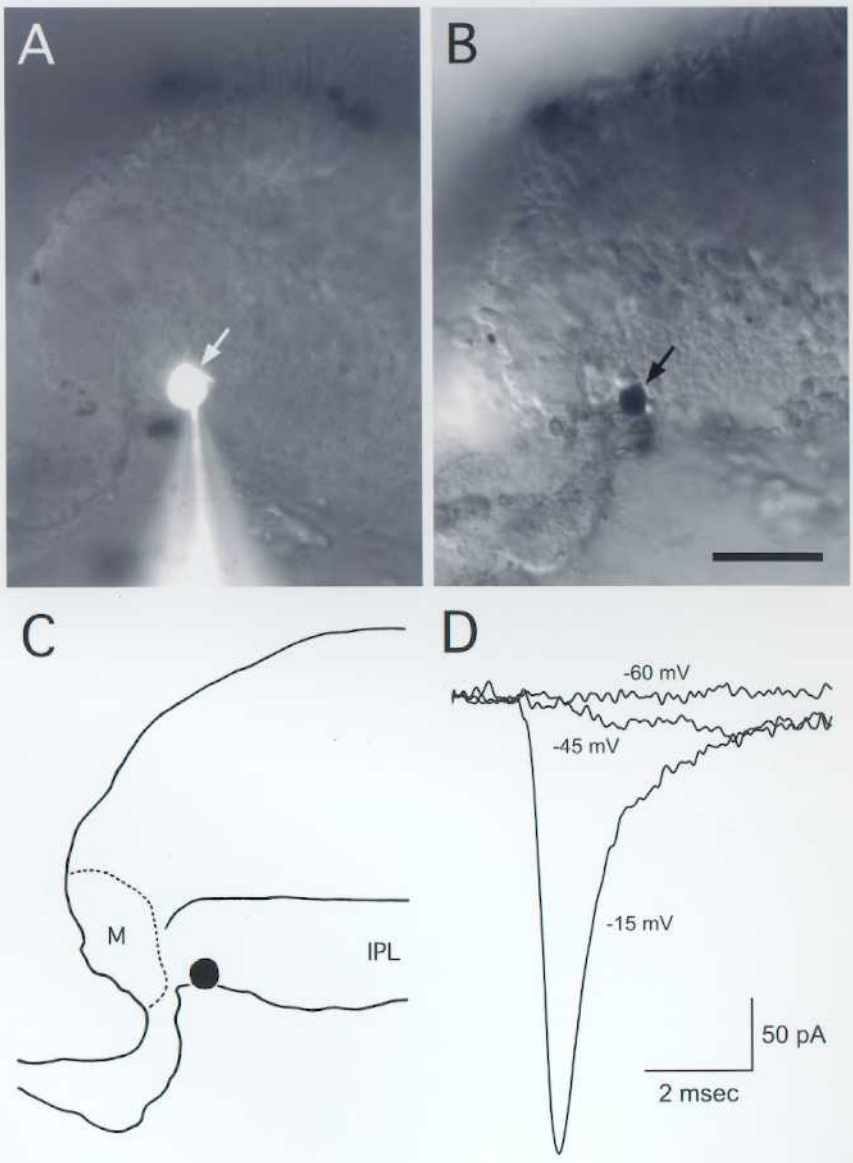
A
B
C
D
M
IPL
-60 mV
-45 mV
-15 mV
50 pA
2 msec